كلية الهندسة بشبرا
FACULTY OF ENGINEERING AT SHOUBRA
ERJ
PRINT ISSN 3009-6049
ONLINE ISSN 3009-6022

ENGINEERING RESEARCH JOURNAL (ERJ)
Volume (53),Issue (4)
October 2024, pp:68-80
https://erjsh.journals.ekb.eg

Surface Water Protection against Oil Spills using Polymeric Nanocomposites Sorbents

Engy Khaled Hassan [1, *], Alaa Elhazek [1], Mohamed Ghobashy [2]

[1] *Civil Engineering Department, Faculty of Engineering at Shoubra, Benha University, Egypt*
[2] *Polymer Chemistry and Nanotechnology Department, Authority of Atomic Energy, Egypt*
**Corresponding author*

E-mail address : engy.city2019@gmail.com , alaa_elhazek@yahoo.com , mohamed_ghobashy@yahoo.com

Abstract: Surface water pollution is increasing greatly due to many factors, including the oil industry. Some causes of pollution with oil are ship accidents, storage tanks, and oil pipelines. This study aims mainly to control, contain, and eliminate the oil spills spread on surface water as quickly as possible to minimize hazards to people, properties, and natural resources. An effective method to achieve this goal is to apply floating barriers (socks) filled with polymer sorbents. Four polyurethane foams (PUF) and their nanocomposites were developed as sorbents for oil spills. These prepared sorbents are eco-friendly, cost-effective, protect surface water resources, and improve local waste-to-resource recycling. Seven different oils were employed. The properties of the developed nanocomposites and their capability to recover absorbed different types of oil were evaluated and achieved significant results. The adsorption capacities were studied as a function of adsorption time, from 5 to 30 minutes. It was concluded that the uptake rate was rapid within the first 5 minutes for all nanocomposites, and then it increased gradually with increased time. Regression analyses were performed developing equations to relate the adsorption capacity and the time. Finally, a viable model of sorption sock was developed and tested successfully. The developed PU foam nanocomposites respond well to oil product spills on the water surface, which can reduce the time for containment.

Keywords: oil spill, oil contamination, sorbents, polyurethane foams, absorbent sock.

1. Introduction

Oil spills may have varying impacts from minimum to large-scale mortality within a specific biological community. Oil spills cause serious threats to fresh water and marine environments, affecting surface and subsurface resources including human food resources.

Weathering can distribute oil spills throughout the water and reduce oil toxicity. Recovery times after oil spills vary from a few days to decades according to the type of environment, the size and type of the spill, and conditions at the time. There is no clear relationship between the size of a spill and the extent of the damage caused. Sometimes natural breakdown of the oil is preferable and more effective.

Polluted surface water is unsafe for drinking, agricultural, and industrial uses. The pollution is increasing greatly with the expansion of the oil industry. Ship accidents, storage tanks, oil pipelines, and oil-contaminated runoff are common sources of oil pollution [1-2]. When oil spills into water, toxic chemicals combine with the water and stay for long periods. For example, a pipeline of liquid diesel fuel was broken in 2008 by accident at South Cairo Helwan's Electrical Station, and the liquids were diverted to the Nile water. This caused an oil spot with a surface area of about 5 Km2 and spread 7 Km apart, [3].

Several methods are considered to minimize the negative impacts of oil spills to protect the environment. These methods are classified as physical/mechanical, chemical, and biological [4-6]. Many variables affect the pollution impacts of a spill and the response methods such as oil type, spill rate, location, and weather conditions. One of the effective methods for eliminating oil spills from water is to apply polymer sorbents [7]. The sorbents include natural organic, natural inorganic, and synthetic. The group of natural organic includes grass, peat moss, sawdust, and corncobs according to oil [8]. Natural inorganic sorbents include argyle, perlite, fur, sand, and volcanic ash. Synthetic sorbents include chemically modified plastic-like materials such as polyurethane, polyethylene, polypropylene, and nylon fibers, [9].

Many synthetic sorbents can absorb many times their weight, [10]. Some synthetic sorbents cannot be cleaned after use, so they can be used against lower-viscosity oils, [11]. Thus, in oil spill treatment, it is important to develop economic sorbent materials of hydrophobic/oleophilic characteristics to improve oil sorption capacity and recovery capability [4, 7, 12]. Polyurethane (PU) is a natural material having properties such as low density, high porosity, easy fabrication, and industrial production [13-14]. It absorbs both oils and water [13-17].

Polyurethane foam (PUF) has high porosity which is ideal for great oil uptake capacity. It is important to improve the sorption capacity of PU foam without decreasing its density. Recent studies have focused on employing PU pores'

surfaces to improve oil swelling capacity [18]. Introducing functional nanomaterials on the surfaces of PUF combined the advantages of both functional nanomaterials and PUF.

Carbon nanotubes (CNTs) were employed as an oil-absorbing material due to their 3D network structures, low density, good mechanical properties, and excellent chemical and thermal stability [19-20]. CNTs/PUF hybrids were developed to improve the oil absorption properties of PUF and can be applied in oil-water treatment. Also, materials with superhydrophilicity and superoleophobicity were employed to separate water from oil/water mixtures [21]. Due to their significant properties, hematite iron oxide (Fe_2O_3) nanoparticles have been widely used in water treatment, pigments, biomedical, lithium-ion batteries, and storage media [22-24].

In this study, four PU foam nanocomposites were developed. Their capability to absorb seven types of oil from water was evaluated.

2. MATERIALS

The chemical compounds used in this paper were conducted by different international companies with high-purity grades (Aldrich, Merck, and Adwic).

2.1 Synthesis Processes

In this study, four nanocomposites were synthesized to investigate their effect in treating different types of oil spills: Polyurethane foams **(**PUF), PU Foams-Based Multi-walled Carbon Nanotubes (PUF/MWCNTs), PU Magnetized Foams-based (PUF/Fe_3O_4), and PU Magnetized Foams-based Multi-walled Carbon Nanotubes (PUF/Fe_3O_4/MWCNTs), as shown in Figure 1.

All Polyurethane foams were synthesized by vigorously mixing components A (MDI oligomers) and B (polyether polyols) in a 2:1 ratio, as shown in Figure 2. After 30 seconds, the mixture was left free to foam.

To synthesize (PUF/MWCNTs), (PUF/Fe_3O_4), and (PUF/Fe_3O_4/MWCNTs) nanocomposites, the multi-walled carbon nanotube (MWCNTs), the iron oxide (Fe_3O_4), and both Fe_3O_4 and MWCNTs each 3% of the weight were suspended in Dimethyl formamide and sonicated for 5 minutes, respectively. They were then added to component A and mixed vigorously. Subsequently, component B was poured into the mixing container, and after 30 seconds the mixture was left free to foam.

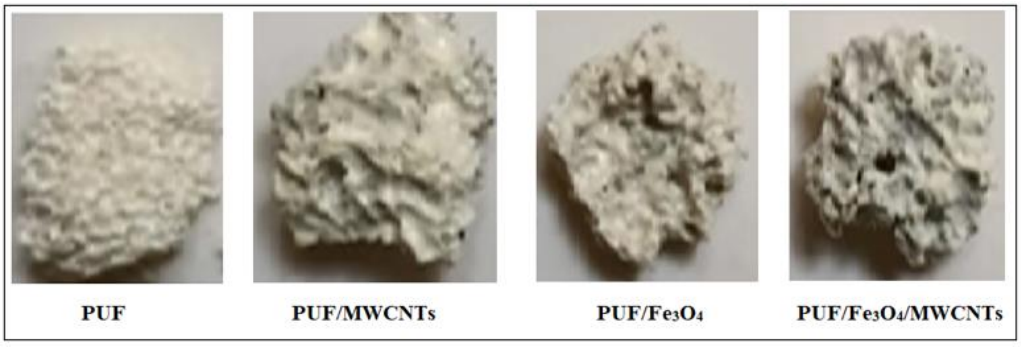

FIGURE 1. Employed Four PU Nanocomposites

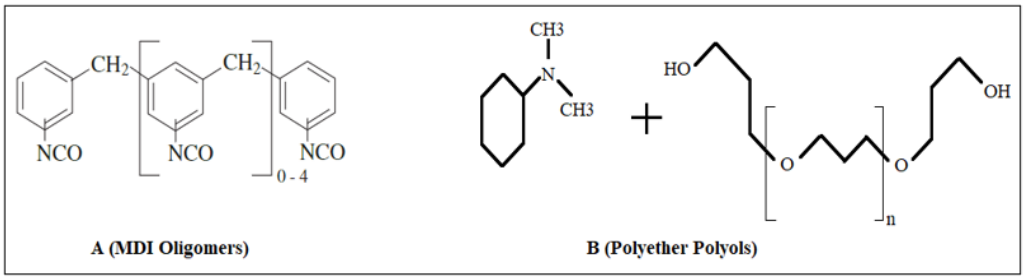

FIGURE 2. Components A (MDI Oligomers) and B (Polyether Polyols)

2.2 Materials Characterization

2.2.1 Fourier Transform Infrared (FT-IR)

FT-IR spectra of the synthesized PU foam showed that the characteristic peaks of PU were close to 3340 cm^{-1}, as shown in Figure 3 (a). These peaks belong to the corresponding vibration of the hydroxyl functional group O–H. The peaks near the wave number of 2973 cm^{-1} were associated with the vibration of –CH_2 and –CH functional groups in the carbonic chains. Also, the PU had a strong intensity of the bands from 900 to 1300 cm^{-1}, indicating the presence of the NCO/OH with the absence of the band around 2250 cm^{-1} of the isocyanate groups -NCO, referring to completing the reaction and consuming all amount of the MDI. The stretching vibration of N–H showed peaks at 2973 cm^{-1} and 2880 cm^{-1} relating to the symmetric and asymmetric stretching vibration

of CH_2 groups. The characteristic band at 1231 cm^{-1} was ascribed to the C–O stretching vibration, [13].

In the FT-IR spectrum of PUF/ MWCNT**s** nanoparticles, as shown in Figure 3 (b), the bands in the 3380-3330 cm^{-1} range can be assigned to the symmetric and asymmetric stretching vibrations of the N-H. The wide peak at 3415 cm^{-1} correlated with hydroxyl O-H groups stretching vibration peak. The C-H stretching vibration was observed at 2972 cm^{-1}, and the strong band stretching vibration at 1230 cm^{-1} was due to C-O-C. The absorption peaks at 1169, 1012, 815, and 758 cm^{-1} were associated with the bending vibration of the C-H bond. The -CH_2 bending vibration, -CH_3 bending vibration, and -CH_2 wagging vibration appeared around 1409, 1400, and 1299 cm^{-1}, respectively.

In the FT-IR spectrum of Fe_2O_3 nanoparticles, as shown in Figure 3 (c), the vibrational bands of Fe–O were recorded at 434 and 541 cm^{-1}, and these peaks slightly shifted in the nanocomposites due to the interaction between Fe_3O_4 with PU. The typical peak of the C=O functional group, NH out-of-plane bending vibration, C–O stretching vibration, and the stretching vibration of N–H were observed with low intensity and shifted to the lower frequencies in the presence of these nanoparticles.

In the FT-IR spectrum of PUF/Fe_3O_4/MWCNTs nanoparticles, as observed in Figure 3 (d), there was an interaction between the oxygen of the Fe_3O_4 and MWCNTs nanoparticles with the NH of the urethane's bond forming complexes that shifted the records.

In the FT-IR spectrum of synthesized Fe_3O_4 nanoparticles, as shown in Figure 3 (e), the band at 541 cm^{-1} was defined as the typical stretching vibration of Fe–O and confirmed the presence of nanoparticles in the synthesized samples [22]. Also, it was shifted to the higher wave numbers in the nanocomposites due to the interaction of Fe_3O_4 nanoparticles with PUF. The vibration of magnetite iron oxide nanoparticles came around 1624 cm^{-1}, confirming the hydrogen bonding between oxygen molecules in iron oxide nanoparticles.

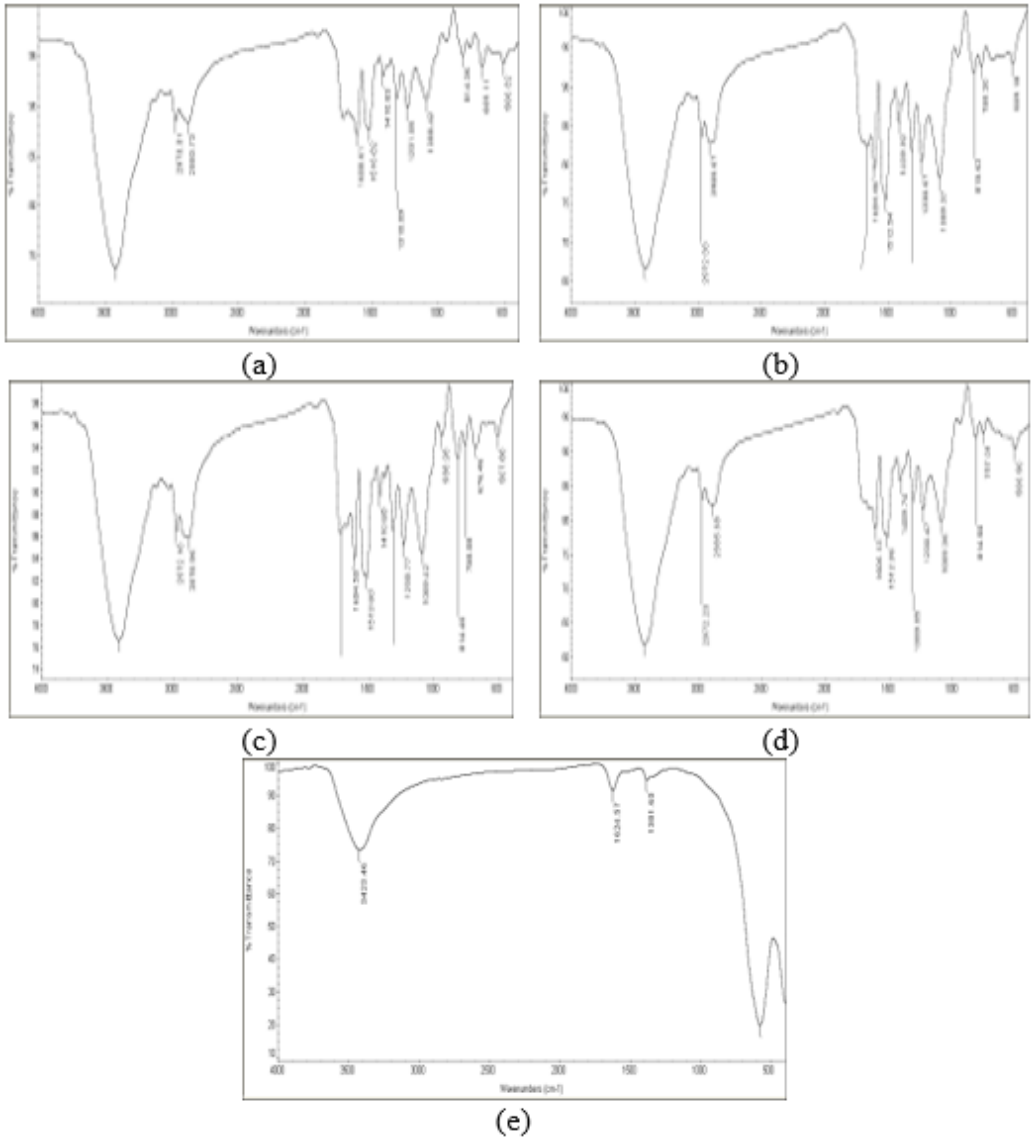

FIGURE 3. Infrared Spectroscopy for **(a)** Polyurethane Foams (PUF), **(b)** PUF/ MWCNT**s**,**(c)** PUF/Fe3O4, **(d)** PUF/Fe3O4/MWCNTs, and **(e)** Fe3O4

2.2.2 Raman Spectroscopy

Typical Raman spectroscopy of MWCNT is shown in Figure 4 (a) with the peaks 1307–1605 cm^{-1}, which is known as the disorder band due to scattering from carbon-containing defects. It appeared precisely at 1307 cm^{-1}. Typical Raman spectroscopy of PUF/MWCNTs is shown in Figure 4 (b) where there was a sharp change in the intensity and sharpness of the band after modification with PUF. The appearance of the band showed a less ordered structure. There was a visible trend in the spectral position of the G-band before and after the reaction with PUF. The untreated nanotubes showed a G-band peak at 1605 cm^{-1}, whereas in polymer-treated samples the band was shifted to a higher wave number of 1613 cm^{-1}. Raman spectroscopy allows checking the Fe_3O_4, PUF/Fe_3O_4, PUF/Fe_3O_4/MWCNTs nanocomposites samples structure, as shown in Figure 4 (c, d, and e), where the magnetic nanoparticles Fe_3O_4 revealed Raman bands from 141–206 cm^{-1} to 666–677 cm^{-1} confirming their structure in nano size. Whereas, in polymer-treated samples, the band was shifted to a higher wave number of 1614 cm^{-1} due to strong adsorption of the PUF to Fe_3O_4.

2.2.3 X-ray Diffraction (XRD)

The X-ray diffraction (XRD) patterns of powder samples under ambient conditions were employed to investigate nanocomposite samples. Figure 5 (a) shows that the polyurethane foam (PUF) with the lowest crystallinity diffraction peak was visible at higher 2θ angles (around 23◦) on the recorded diffractogram, which reflected delaminated structures. Figure 5 (b, c, and d) shows that there was a maximum peak at 19.25◦ concerning PUF/MWCNTs, PUF/Fe_3O_4, and PUF/Fe_3O_4/MWCNTs nanocomposites due to the interaction of PUF with these nanofillers that reduced its intensity. The XRD of Fe_3O_4 is shown in Figure 5 (e) exhibiting six distinct diffraction peaks at 2θ values of 30.3°, 35.5°, 43.2°, 53.5°, 57° and 62.7°, which correspond to the 220, 311, 400, 422, 511, and 540 crystallographic planes of the inverse spherical magnetite crystal.

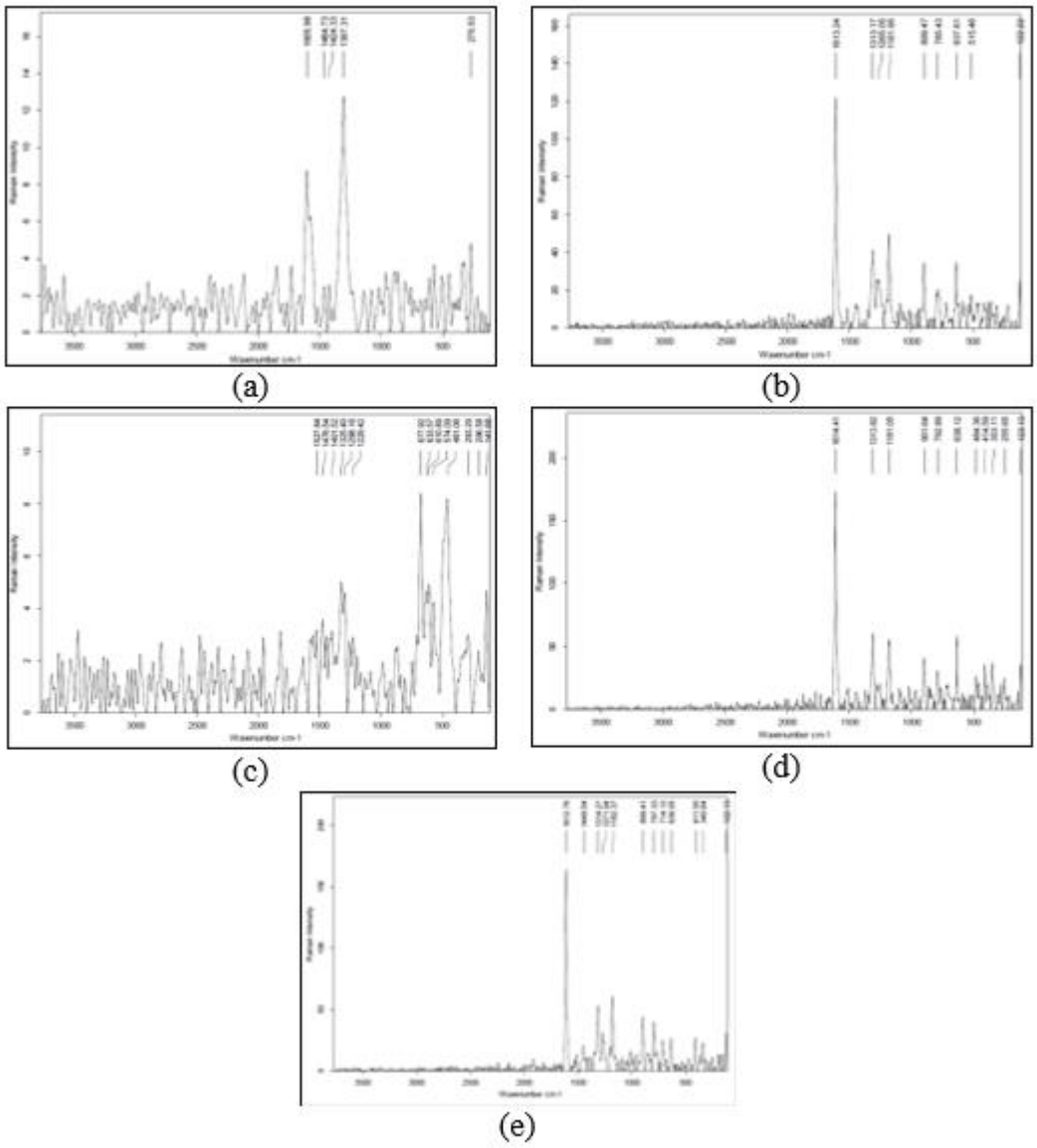

FIGURE 4. Raman Spectroscopy for **(a)** CNTs**, (b)** PUF/CNTs, **(c)** Fe3O4, **(d)** PUF/Fe3O4, and **(e)** PUF/CNTs/Fe3O4

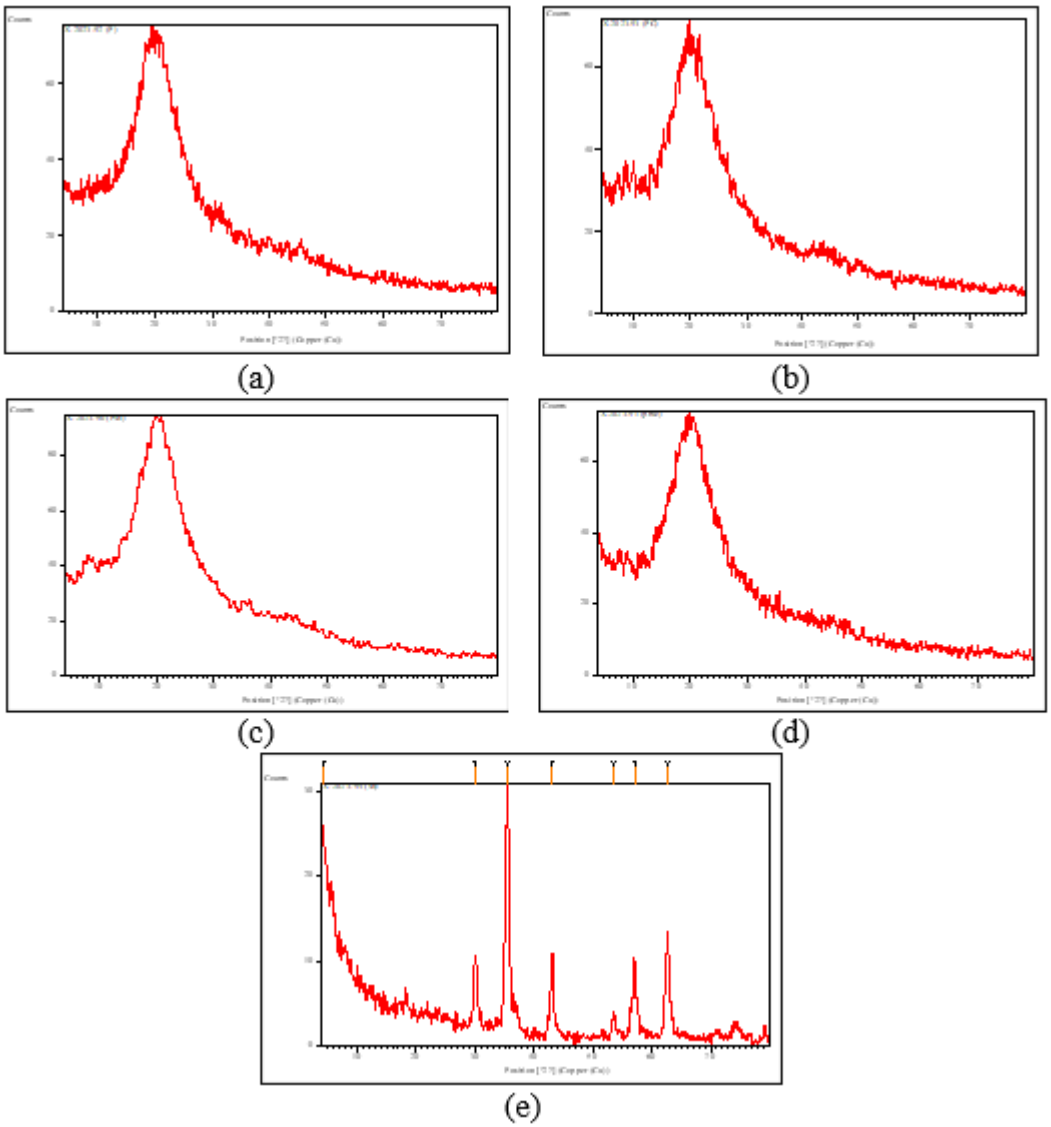

FIGURE 5. Raman Spectroscopy for **(a)** PUF**, (b)** PUF/MWCNTs**, (c)** PUF/Fe3O4**,(d)** PUF/Fe3O4/MWCNTs, and **(e**) PUF/CNTs/Fe3O4

2.2.4 Dynamic Light Scattering (DLS)

DLS analysis results showed different particle size distributions of nanoparticles. A discrepancy in the size of nanoparticles was revealed, where the dynamic light scattering method gives the hydrodynamic diameter rather than the actual diameter of nanoparticles. As shown in Figure 6, the mean hydrodynamic particle diameter was 204 nm for the particle size of each PUF/MWCNTs and PUF/ Fe_3O_4/MWCNTs. The mean hydrodynamic particle diameter was 275.1 for Fe_3O_4. The peak particle size distributions of the PUF/Fe_3O_4 and MWCNTs were 142.4 and 702.5 nm.

2.2.5 Transmission Electron Microscopy (TEM)

The particle size of the samples was determined by transmission electron microscopy (TEM). A few quantities of nanocomposite and nanoparticles were dispersed in 10 mL ethanol and sonicated for 30 minutes. A few drops of the resulting suspension were placed on a covered copper grid. MWCNTs had smooth surfaces and integrated hollow tubular structures. Most impurity phases, such as amorphous carbon and graphitic nanoparticles, were removed. The diameter of the MWNTs was 20–30 nm.

2.3 Dynamic Viscosity and Density

In this study, seven different oils were employed: crude oil, motor oil, crude oil (I), crude oil (II black), pump oil, crude oil (III), and castor oil. Density, specific gravity, API gravity, and dynamic viscosity were measured according to standard methods, as shown in Table 1.

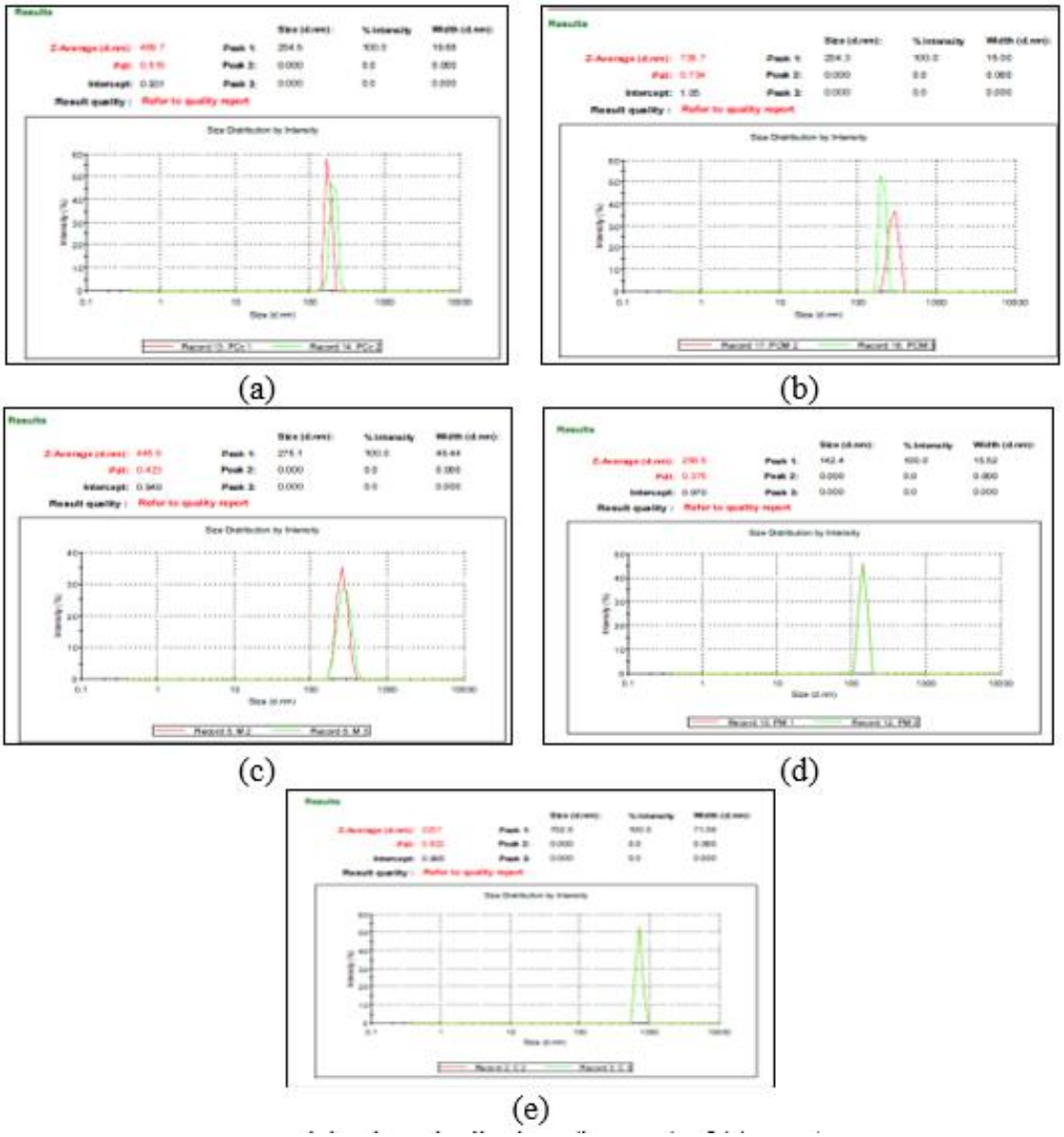

FIGURE 6. Particle Size Distributions (by DLS) of **(a)** PUF/MWCNTs**,(b)** PUF/ Fe3O4/MWCNTs, **(c)** Fe3O4**, (d)** PUF/Fe3O4, **and (e)** MWCNTs

TABLE 1. Analyses of Oil Samples

No	Type of Oil	ASTM D-4052			ASTM D-445
		Density at 15.56 °C, kg/m^3	Specific Gravity	API gravity at 60 °F, °API	Dynamic Viscosity at 40^o C, cP
1	Crude Oil	0.9059	0.9068	24.54	172.57
2	Motor Oil	0.8873	0.8882	27.81	148.90
3	Crude Oil I	0.7575	0.7583	55.10	0.53
4	Crude Oil II	0.8983	0.8990	25.90	23.43
5	Pump Oil	0.8403	0.8416	36.72	12.81
6	Crude Oil III	0.9376	0.9385	19.27	152.03
7	Castor Oil	0.9643	0.9653	15.09	243.34

3. EXPERIMENTAL TECHNIQUES

Oily water treatment was performed by the oil adsorption method [7, 14, 20], and the oil residue was estimated by the gravimetric method [4, 7].

The general steps for each experiment are:

1) Each used oil of 1.0 g/L was placed in Petri dishes that contained 20 mL water.
2) A quantity of 0.02 g/L of the prepared PUF was added into the suspension, and left for a contact time of 1 minute to 24 hours, maintaining a pH value of 7 to obtain the best condition for the aqueous solution.
3) The proceedings were made at room temperature (30 ± 1 °C), and the mixtures reached their high rapturous state using a mechanical shaker.
4) The samples were taken off, and the oil was separated and calculated using a rotary evaporator and weighing the resulting oil residue.

The same previous steps were repeated for the three other nanocomposites: PUF/MWCNTs, PUF/Fe3O4, and PUF/Fe3O4/MWCNTs.

Also, the same previous steps were repeated for each of PUF, PUF/MWCNTs, PUF/Fe3O4, and PUF/Fe3O4/MWCNTs nanocomposites using waste oil and crude oil (III) with contact times: 0, 5, 10, 15, 20, and 30 minutes.

4. RESULTS AND DISCUSSIONS

4.1 Density and Viscosity Effect on Adsorption Process

Due to capillary force, oil is absorbed in the pores of the superhydrophobic PUF and fills the pores. Oil is also adsorbed on the outer surface of the foams due to the hydrophobic force. As the density of the oil increases, the amount of oil that can be stored per unit volume of the PUF composite increases. Also, the high viscosity prevents oil from diffusing into the internal pores of the adsorbent causing ineffective oil capture, [25]. Some researchers have shown that sorbents are more effective on liquid oils with lower viscosity, [26-27]. The captured oil may be prevented from being washed away from the sorbent materials owing to high viscosity.

4.2 Adsorption Performance of the Nanocomposites for Different Oils

In this study, hydrophobic polyurethane foam was prepared via foaming technology. The prepared PUF foams could quickly and selectively adsorb various types of oils, and a simple squeezing process could collect the adsorbed oils. PUF, PUF/MWCNTs, PUF/Fe3O4, and PUF/Fe3O4/MWCNTs nanocomposites achieved effective oil-water adsorption due to their superhydrophobic/superoleophilic properties, as shown in Figures 7 and 8.

The results proved significant adsorption capacities employing nanocomposites for different oils in most cases, as illustrated in Tables 2 and 3. As tabulated in Table 4, BUF has maximum adsorption capacity for 6 of the 7 used oils. Only motor oil is associated with low adsorption capacity when employing BUF while using PUF/Fe3O4/MWCNTs and PUF/MWCNTs achieved significant adsorption capacity.

The adsorption capacities are varied due to the oils' different viscosity, density, and other properties. This has been previously reported for other sorbents, [28]. Powdered activated carbon was employed as sorbent for crude oil, where the treated samples were stirred with a magnetic stirrer for different contact time intervals and filtered through filter papers, [29], achieving adsorption capacity 2. Lawsonia plant leaves were used as a natural adsorbent in the oil spill cleaning from seawater achieving a sorption uptake of 1.60, [30]. In this paper, an adsorption capacity of 2.39 was achieved using BUF.

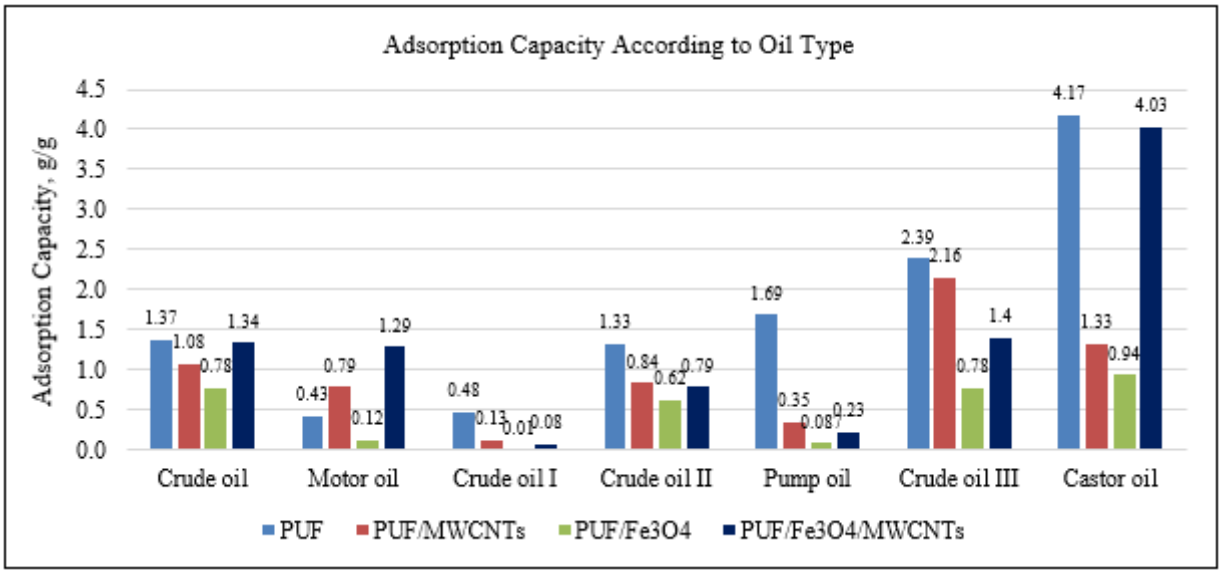

FIGURE 7. Adsorption Capacity According to Oil Type

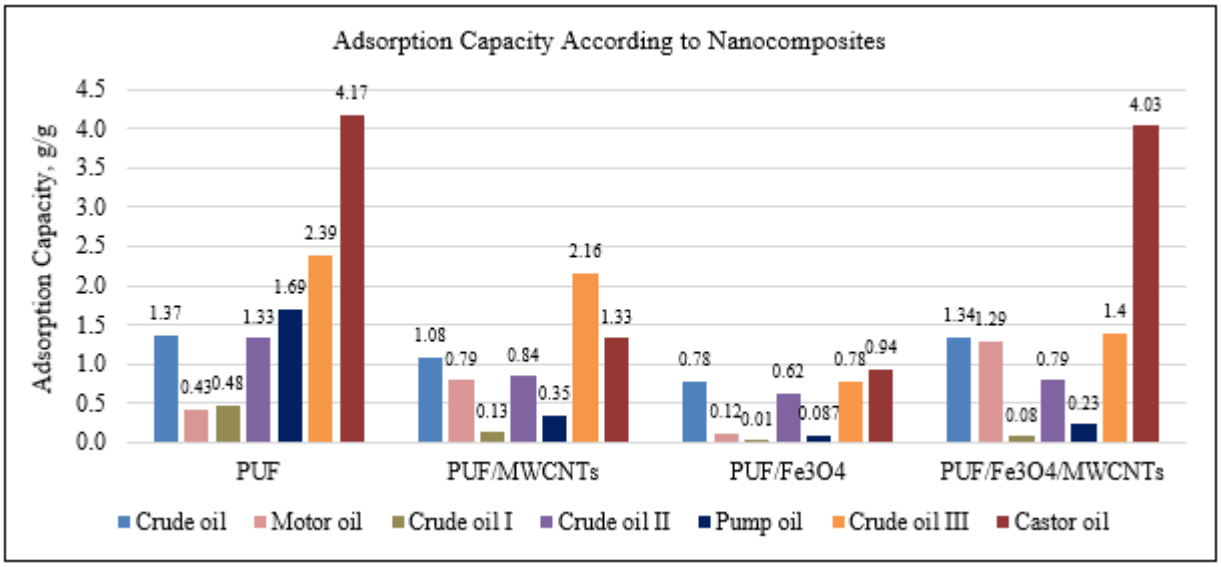

FIGURE 8. Adsorption Capacity According to Nanocomposites

TABLE 2. Effect of the Used Nanocomposites

Oil Type	Max and Min Adsorption Capacities, g/g	Effect Order of the Used Nanocomposites			
		PUF	PUF/MWCNTs	PUF/Fe_3O_4	PUF/Fe_3O_4/ MWCNTs
Crude oil	1.37 & 0.78	1st	3rd	4th	2nd
Motor oil	1.29 & 0.12	3rd	2nd	N*	1st
Crude oil I	0.84 & 0.01	1st	N*	N*	N*
Crude oil II	1.33 & 0.62	1st	2nd	4th	3rd
Pump oil	1.69 & 0.09	1st	2nd	N*	N*
Crude oil III	2.39 & 0.78	1st	2nd	4th	3rd
Castor oil	4.17 & 0.94	1st	3rd	4th	2nd

N*: Not significant

TABLE 3. Effect on the Used Oils

Nanocomposite	Max and Min Adsorption Capacities, g/g	Effect Order on the Used Oils						
		Crude oil	Motor oil	Crude oil I	Crude oil II	Pump oil	Crude oil III	Castor oil
PUF	4.17 & 0.43	4th	7th	6 th	5th	3rd	2nd	1st
PUF/ MWCNTs	2.16 & 0.13	3rd	5th	N*	4th	6th	1st	2nd
PUF/Fe_3O_4	0.94 & 0.01	2nd	N*	N*	4th	N*	3rd	1st
PUF/Fe_3O_4/MWCNTs	4.03 & 0.08	3rd	4th	N*	5th	N*	2nd	1st

N*: Not significant

4.3 Effect of Time

The effect of time on the adsorption capacities of foam nanocomposites samples (PUF, PUF/MWCNTs, PUF /Fe_3O_4, and PUF/Fe_3O_4/MWCNTs) was studied for 2 oils (crude oil and crude oil III).

To investigate the uptake of crude oil and crude oil III from the oil-water mixture by concentration (5 g\L) at pH 7, the adsorbed amount per gram of the absorbents was studied as a function of contact time, from 5 to 30 min. It was concluded that the uptake rate of crude oil and crude oil III was rapid within the first 5 min for all nanocomposites, then it increased gradually with increased time.

As shown in Figure 9, the adsorption rate for crude oil achieved 1.53, 2.09, 1.52, and 0.91 times the initial weight of PUF, PUF/MWCNTs, PUF/Fe_3O_4, and PUF/Fe_3O_4/MWCNTs nanocomposites in first 5 min.

As shown in Figure 10, the adsorption rate for crude oil III reached 2.85, 2.25, 1.89, and 2.71 times the initial weight of PUF, PUF/MWCNTs, PUF/Fe_3O_4, and PUF/Fe_3O_4/MWCNTs nanocomposites in first 5 min.

Regression analyses were performed developing equations to relate the adsorption capacity and the time, as illustrated in Figures 9 and 10.

These results indicate that the significant time for the adsorption process was 5 min, which is considered sufficient time for the adsorption of crude oil and crude oil III from the water surface under the operating conditions used.

4.4 Adsorption Process

From the experiments done in this study, the nanocomposite samples before and after adsorbing crude oil from water are shown in Figure 11. The progress in the adsorptive capacity of crude oil and crude oil III from water within 30 min is shown in Figure 12.

Table 4. Adsorption Capacity and Relative Adsorption Capacity w.r.t. BUF

Oil Type	PUF	PUF/MWCNTs		PUF/Fe_3O_4		PUF/Fe_3O_4/MWCNTs	
	Adsorption Capacity, g/g	Adsorption Capacity, g/g	Relative Adsorption Capacity, %	Adsorption Capacity, g/g	Relative Adsorption Capacity, %	Adsorption Capacity, g/g	Relative Adsorption Capacity, %
Crude oil	1.37	1.08	-21.17	0.78	-43.07	1.34	-2.19
Motor oil	0.43	0.79	83.72	0.12	-72.09	1.29	200.00
Crude oil I	0.48	0.13	-72.92	0.01	-97.92	0.08	-83.33
Crude oil II	1.33	0.84	-36.84	0.62	-53.38	0.79	-40.60
Pump oil	1.69	0.35	-79.29	0.09	-94.67	0.23	-86.39
Crude oil III	2.39	2.16	-9.62	0.78	-67.36	1.40	-41.42
Castor oil	4.17	1.33	-68.11	0.94	-77.46	4.03	-3.36

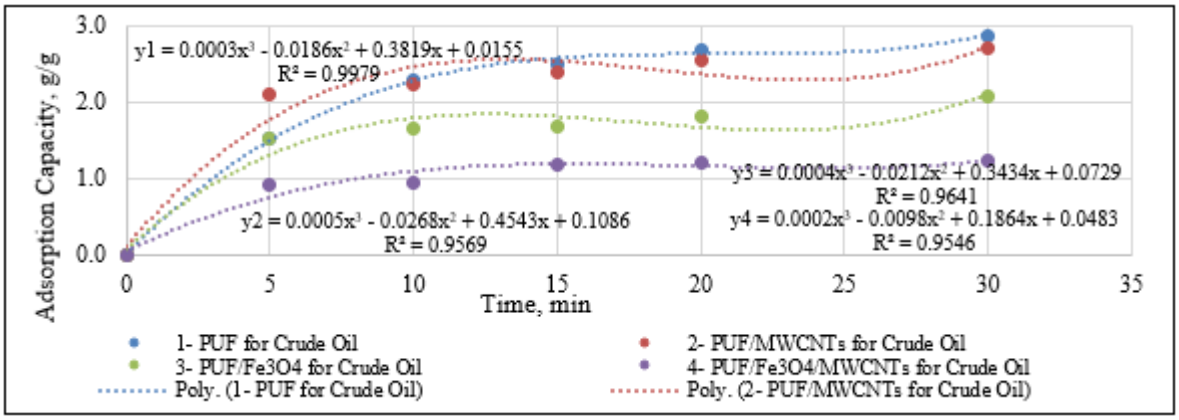

FIGURE 9. Adsorption Capacities of Nanocomposite Samples with Crude Oil vs. Contact Time

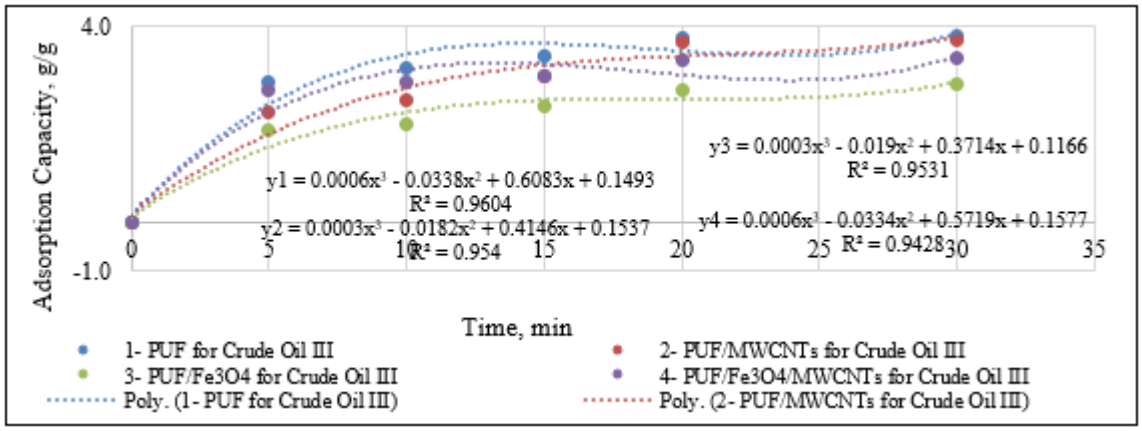

FIGURE 10. Adsorption Capacities of Nanocomposite Samples with Crude Oil III vs. Contact Time

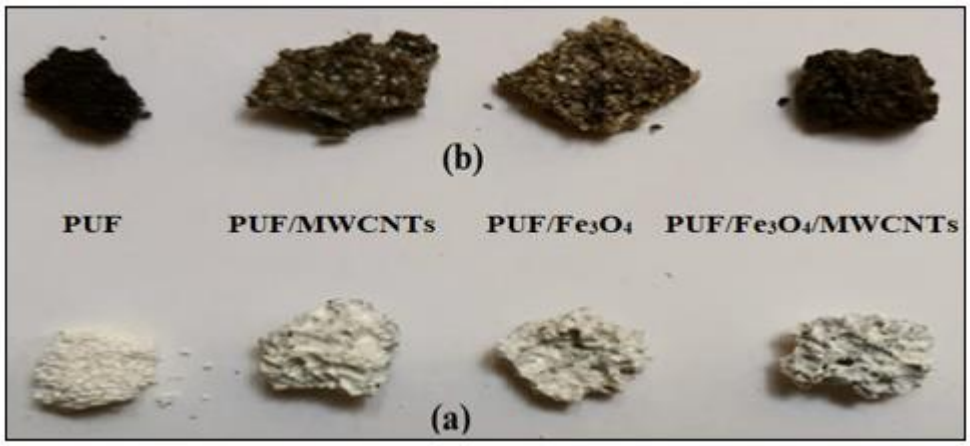

FIGURE 11. Nanocomposites Samples (**a)** Before and **(b)** After immersing in Oil/Water Mixture for 30 min

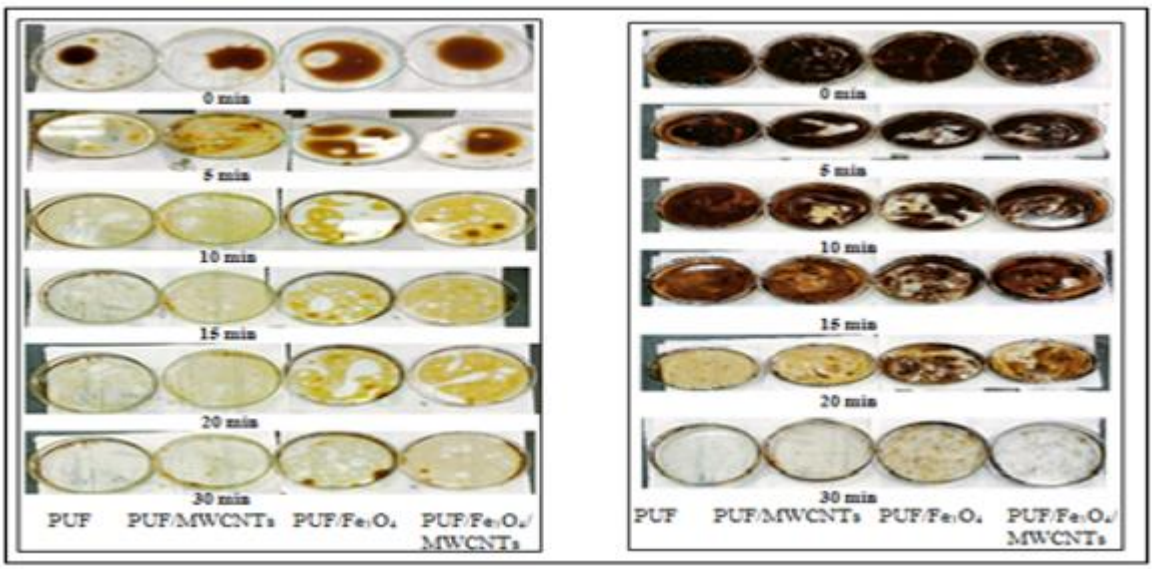

FIGURE 12. Adsorption Processes of Crude Oil and Crude Oil III from Water

4.5 Developed Model (PROTOTYPE)

The sorption socks, also called the snakes, consist of the inclusion action (booms) and the oil contamination collecting action (sorbents). They have two types of adsorbents; the first adsorbent is the textile cover of the sorption sock, and the second represents the filling that can be any loose sorbent.

The sorption snakes are used for solving the problem of oil spills in rivers, streams, lakes, ponds, etc., and also for use on solid surfaces. Their main function is to contain the oil spill to avoid contamination spread to a larger area. Sorption socks can be designed differently such as long with a small diameter or short with a large diameter.

In this study, a prototype (sorption sock filled with PUF mixed with sand) was developed and tested. The cover was tested alone as the first adsorbent, and the filling was examined as the second adsorbent. All used materials were tested for the absorption of oil and water/oil mixtures. The significant results of the PUF nanocomposites are because of the hydrophobic, or water-repellent, quality that permits them to be used for clearing up oil spills from ponds, streams, water tanks, and pools without the pads and socks becoming a soggy, waterlogged mess. They will not sink in water even if saturated with oil. The developed model and its cross-section before and after immersing in the oil/water mixture are shown in Figures 13 and 14.

FIGURE 13. Developed Model **(a)** before and **(b)** after immersing in Oil/Water Mixture

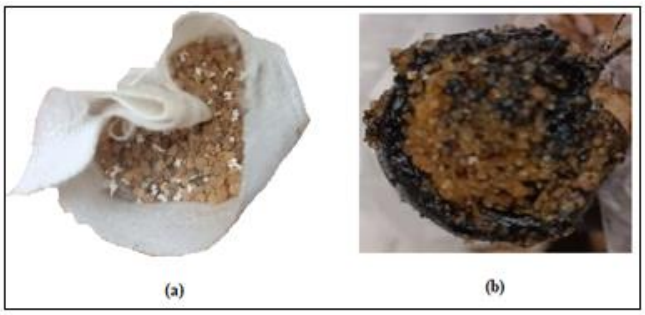

FIGURE 14. Cross-Section of the Developed Model **(a)** before and **(b)** after immersing in Oil/Water Mixture

The sorption efficiency of oil removal using the developed model is illustrated in Figure 15 demonstrating the recovery stages of an oil spill on the water surface after immersing the model in it for 30 min.

The white absorbent socks change their color as the oil is sucked up, so it's obvious when the material has to be disposed of. The reusability of PU foam is determined by repeating the oil/water adsorption/desorption of the nanocomposites for 10 cycles.

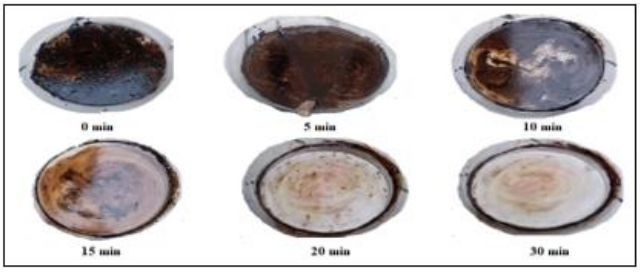

FIGURE 15. Removal Stages of Oil Spill on Water Surface using the Developed Model

4.6 Continuous Oil Removal

The oil removal process can be disrupted due to turbulence caused by strong winds and waves. A continuous oil removal system can be employed to overcome this challenge.

In this study, a continuous oil removal experiment was done by applying a PUF sample to an oil collection vessel, as shown in Figure 16.

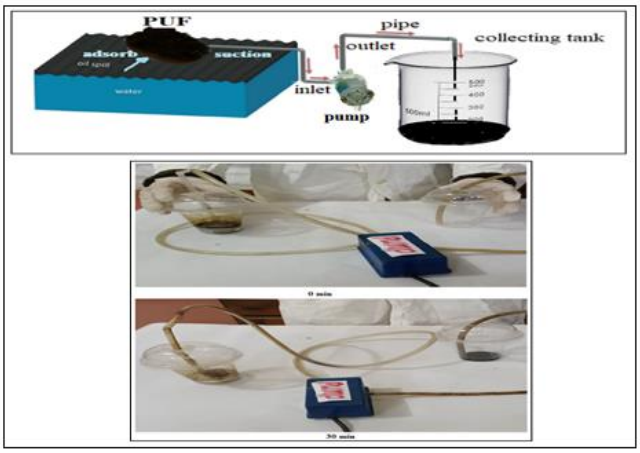

FIGURE 16. Continuous Oil Removal Experiment

When the sorbent is placed over a spill area, the oil is drawn into the pores by capillary force until the sorbent is fully saturated. The following pumping action aims to lower the oil pressure near the pump nozzle. As oil is removed from the PUF, the material's pores begin to fill up with air, preventing water penetration into the sorbent material, [31].

5. CONCLUSIONS

For crude oil, motor oil, crude oil I, crude oil II, pump oil, crude oil III, and castor oil; it was concluded that the adsorption capacities employing different nanocomposites ranged between (1.37 and 0.78), (1.29 and 0.12), (0.84 and 0.01), (1.33 and 0.62), (1.69 and 0.09), (2.39 and 0.78), and (4.17 and 0.94) times their initial weight, respectively.

The studied 4 nanocomposites were significantly effective for crude oil, crude oil II, crude oil III, and castor oil. The 3 other oils were affected only by applying 1 or 2 or 3 of the used nanocomposites.

PUF was significantly effective for all 7 different oils.
PUF/MWCNTs were significantly effective for 6 of the 7 different oils.
PUF/Fe_3O_4 was significantly effective for 4 of the 7 different oils.
PUF/Fe_3O_4/MWCNTs was significantly effective for 5 of the different 7 oils.

It was concluded that PUF is significantly effective against crude oil, crude oil I, crude oil II, pump oil, crude oil III, and castor oil.

It was also concluded that PUF/Fe_3O_4/MWCNTs are significantly effective against motor oil.

It was concluded that the rate of uptake of crude oil and crude oil III was rapid within the first 5 min for all nanocomposites, and then it increased gradually with increased time.

Equations were developed to relate the adsorption capacity and the time.

It is recommended to evaluate the sock's performance in real-world scenarios and a cost analysis.

It is recommended to study the environmental impact of the continuous oil removal process.

More sorbents and oil-collecting devices based on factors such as high efficiency, good biodegradation, easy fabrication, low cost, good ability of reuse and recovery, and facilitated application should be developed.

Furthermore, the management strategy of post-used sorbents and the treatment of collected oil should be further investigated to avoid secondary environmental pollution and enhance the performance of sorbents and oil collection devices.

References

[1] Akhtyamov R, Titova T S, Glazkov D V, and Gavrilin I I (2021). "Protection of water supply sources from the emergency oil spill on the water surface". IOP Conf. Ser.: Earth Environ. Sci., 937. Doi:10.1088/1755-1315/937/3/032026

[2] Poonam Kumari, Kumud Malika Tripathi, Kamlendra Awasthi, and Ragini Gupta (2023). "Biomass-derived carbon nano-onions for the effective elimination of organic pollutants and oils from water". Environmental Science and Pollution Research, Vol. 30. https://doi.org/10.1007/s11356-023-27457-5

[3] Sadek M. E., Seheimy A. E., El-Tokhy T. T., and Allah M. A. (2017). "Management Process of Oil Spill in Water Plants". J Pollut Eff Cont 5: 205.

[4] Abdeen Z., Abdelfattah M. Badawi, Ahmed I. Adawi, Akram M. Eldidamony, Abd el-Shafey I. Ahmed and Eslam Hafez. (2016). "Effect of sonication time on degradation of refinery petroleum wastewater using the prepared cationic silyl polymeric surfactant". ChemXpress 9(1), 030-045.

[5] M. G. Gote, H. H. Dhila, and S. R. Muley (2023). "Advanced Synthetic and Bio-Based Sorbents for Oil Spill Clean-up: A Review of Novel Trends". Nature Environment and Pollution Technology, Vol. 22, No. 1, 39-61.

[6] M. E. Mohamed & B. A. Abd El Nabey (2022). "Fabrication of a biological metal–organic framework based superhydrophobic textile fabric for efficient oil/water separation". Scientific Reports, 12: 15483.

[7] Zizi I. Abdeen and Amin I. Ghoneim. (2020). "Improving of the Mg-Co nano-ferrites Efficiency for Crude Oil Adsorption from Aqueous Solution by Blending them with Chitosan Hydrogel". Environmental Science and Pollution Research journal, 27(16): 19038-19048.

[8] Ezzat M. Soliman, Salwa A. Ahmed & Aliaa A. Fadl (2020). "Adsorptive removal of the oil spill from seawater surface using magnetic wood sawdust as a novel nano-composite synthesized via microwave approach". Journal of Environmental Health Science and Engineering, 18:79–90.

[9] Abeer Alassod, Magdi Gibril, Syed Rashedul Islam, Wanzhen Huang, and Guangbiao Xu (2020). "Polypropylene/lignin blend monoliths used as sorbent in oil spill cleanup". Heliyon 6, e04591

[10] Hadela A, Lakić M, Potočnik M, Košak A, Gutmaher A, Lobnik A. (2020). "Novel reusable functionalized magnetic cobalt ferrite nanoparticles as oil adsorbents". Adsorption Science & Technology. 38 (5-6): 168-190.

[11] Ghalambor A. (1995). "Evaluation and characterization of sorbents in the removal of oil spills". Louisiana Oil Spill Coordinator's Office, Louisiana Applied Oil Spill Research and Development Program, Baton Rouge, Louisiana, OSRADP Technical Report Series, 95-006.

[12] FENG Zhao-xuan, XU Ya-nan, YUE Wei-xun, Karin H. Adolfsson, and WU Ming-bo (2021). "Recent progress in the use of graphene/polymer composites to remove oil contaminants from water". NEW CARBON MATERIALS, Vol. 36 No. 2. DOI: 10.1016/S1872-5805(21)60018-5

[13] Zizi Abdeen. (2015). "Enhanced Recovery of Lead (II) Ions from Aqueous Solutions Using Polyurethane Composite as Adsorbent". Environmental process journal, 2: 189-203.

[14] Mohamed M. Ghobashy and Zizi I. Abdeen. (2016). "Influence of Gamma Irradiation on the Change of the Characterization of Elastomeric Polyurethane". Adv. Sci. Eng. Med. 8, 736–739.

[15] Patalano, A., Villalobos, F., Pena, P., Jauregui, E., Ozkan, C., & Ozkan, M. (2019). "Scaling sorbent materials for real oil-sorbing applications and environmental disasters". MRS Energy & Sustainability, 6, E3.

[16] Salma Elhenawy, Majeda Khraisheh, Fares AlMomani, Mohammad K. Hassan, Mohammad A. Al-Ghouti, and Rengaraj Selvaraj (2022). "Recent Developments and Advancements in Graphene-Based Technologies for Oil Spill Cleanup and Oil–Water Separation Processes". Nanomaterials (Basel). 12(1).

[17] A. Keshavarz, H. Zilouei, A. Abdolmaleki, A. Asadinezhad. (2015). "Enhancing oil removal from water by immobilizing multi-wall carbon nanotubes on the surface of polyurethane foam". J. Environ. Manage. 157.

[18] J. Pinto, A. Athanassiou, and D. Fragouli. (2018). "Surface modification of polymeric foams for oil spills remediation". J. Environ. Manage. 206, 872–889.

[19] T. Zhang, F. Hu, C. Zhang, D. Yang, F. Qiu, and X. Peng. (2017). "A novel multi-wall carbon nanotubes/poly(n-butylacrylate-co-butyl methacrylate) hybrid resin: synthesis and oil/organic solvents absorption". Fiber. Polym., 18.

[20] Zizi Abdeen (2016). "Adsorption efficiency of poly(ethylene glycol)/chitosan/CNT blends for maltene fraction separation". Journal of Environ. Sci. Pollut. Res., 11240-11246.

[21] L. Wu, L. Li, B. Li, J. Zhang, and A. Wang (2015). "Magnetic, durable, and superhydrophobic polyurethaneFe3O4@SiO2@fluoropolymer sponges for selective oil absorption and oil/water separation". ACS Appl. Mater. Interfaces 7, 4936–4946.

[22] Mohamed Mohamady Ghobashy and M.A. Elhady. (2017). "Radiation crosslinked magnetized wax (PE/Fe3O4) nanocomposite for selective oil adsorption". Composites Communications 3, 18–22.

[23] H. Ikram, A. Al Rashid, and M. Koc. (2022). "Synthesis and characterization of hematite (α-Fe2O3) reinforced polylactic acid (PLA) nanocomposites for biomedical applications". Composites C 9, 100331.

[24] H. Aliah, D. G. Syarif, R. N. Imana, A. Sawitri, W. Darmalaksana, A. Setiawan, A. Malike, and P. Gumarang. (2019). "Structure analysis of nanocomposite ZnO: Fe2O3 based mineral yarosite as Fe2O3 source and its application probability". Mater. Today: Proc. 13, 36–40.

[25] Chang J., Shi Y., Wu M., Li R., Shi L., Jin Y., Qing W., Tang C., and Wang P. (2018). "Solar-assisted fast cleanup of heavy oil spills using a photothermal sponge". J. Mater. Chem. A.; 6: 9192–9199.

[26] Feng J., Nguyen S. T., Fan Z., and Duong H. M. (2015). "Advanced fabrication and oil absorption properties of super-hydrophobic recycled cellulose aerogels". Chem Eng J. https://Doi.org/10.1016/j.cej.2015.02.034

[27] Kim H. J., Han S. W., and Kim J. H. (2018). "Oil absorption capacity of bare and PDMS-coated PET non-woven fabric; dependency of fiber strand thickness and oil viscosity". Curr Appl Phys, 18: 369–376.

[28] Yuan D., Zhang T., Guo Q., Qiu F., Yang D., and Ou Z. (2018). "Recyclable biomass carbon@SiO2@MnO2 aerogel with hierarchical structures for fast and selective oil-water separation". Chem. Eng. J.; 351: 622–630.

[29] Khaled Okiel, Mona El-Sayed, and Mohamed Y. El-Kady (2011). "Treatment of oil-water emulsions by adsorption onto activated carbon, bentonite, and deposited carbon". Egyptian Journal of Petroleum (2011) 20, 9–15. doi:10.1016/j.ejpe.2011.06.002

[30] Mohamed A. Mahmoud, Aghareed M. Tayeb, Ahmed M. Daher, Omer Y. Bakather, Mohamed Hassan, Mubarak A. Eldoma, Yasir A. Elsheikh, and Ahmed F.F. Abouatiaa (2022). "Adsorption study of oil spill cleanup from seawater using natural sorbent". Chemical Data Collections, Volume 41, 100896, https://doi.org/10.1016/j.cdc.2022.100896.

[31] Tan J. Y., Low S. Y., Ban Z. H., and Siwayanan P. (2021). "Oil spill clean-up with bio-sorbents". Bio-Resources.; 16(4). DOI: 10.15376/biores. 16.4. Tan.